Wear 326-327 (2015) 20–27

Contents lists available at ScienceDirect

Wear

journal homepage: www.elsevier.com/locate/wear

Effect of contact pressure on fretting fatigue behavior of Ti-1023

G.Q. Wu [a,*], X.L. Liu [a], H.H. Li [a], W. Sha [b], L.J. Huang [c]

[a] School of Materials Science and Engineering, Beihang University, 37 Xueyuan Road, Haidian District, Beijing 100191, China
[b] School of Planning, Architecture and Civil Engineering, Queen's University Belfast, Belfast BT7 1NN, UK
[c] Beijing Institute of Aeronautical Materials, Beijing 100095, China

ARTICLE INFO

Article history:
Received 30 August 2014
Received in revised form
20 December 2014
Accepted 22 December 2014
Available online 31 December 2014

Keywords:
Fretting
Fatigue
Non-ferrous metals
Fracture
Electron microscopy
Wear testing

ABSTRACT

With a new test facility, we have investigated fretting fatigue properties of Ti-1023 titanium alloy at different contact pressure. Both fatigue fracture and fretting scar were analyzed by scanning electron microscopy (SEM). Moreover, the depth of crack initiation area in fatigue fracture has been analyzed quantitatively, to investigate the relationship between the depth of crack initiation area and the fretting fatigue strength. The changing trends of the depth of crack initiation area and fretting fatigue strength with the increase of contact pressure show obvious opposite correlations. The depth of crack initiation area increases rapidly with the increase of contact pressure at low contact pressure (smaller than 10 MPa), and the fretting fatigue strength drops rapidly. At the contact pressure of 10–45 MPa, both the depth of crack initiation area and the fretting fatigue strength do not vary significantly. Contact pressure influences fatigue strength through influencing the initiation of fatigue crack. The main damage patterns are fatigue flake and plow.

1. Introduction

Ti-1023 titanium alloy is widely used in aircraft structural components due to its high specific strength, good fracture toughness, excellent stress corrosion resistance, and enhanced processing characteristics [1,2]. The process known as fretting fatigue occurs at the contact surfaces of two components that have an oscillatory motion of small amplitude, and the relative movement is the consequence of cyclic loading of one of the components. Compared with other alloy kinds, titanium alloys are more susceptible to fretting fatigue, which is a serious failure problem in critical structural components. The reason might be the damage of the protective surface oxide, the deformation or temperature-induced phase transformation and the great tendency for material transfer when rubbing with other materials [3,4]. In most practical applications, titanium alloy components need to be mechanically connected with other components. The connection interface is often under some fretting loading, which easily results in fretting fatigue damage [4]. However, there are few reports on fretting fatigue of Ti-1023 titanium alloy.

Many factors might influence fretting fatigue of titanium alloy: contact pressure, surface condition, slip amplitude, microstructure, etc. Much research has been conducted for understanding influences of various parameters on fretting fatigue strength [5–25]. The main parameters include fretting amplitude, contact pressure, and coefficient of friction [26]. Among the three factors, fretting amplitude is affected by coefficient of friction and contact pressure, and the coefficient of friction has a great connection with inherent properties of materials. So, the largest variable is contact pressure. The effect of contact pressure has been studied by many researchers using various materials and a variety of conclusions have been obtained.

Carbon steel was experimentally investigated by Endo and Goto [27]. 4130 Steel was experimentally investigated by Gaul and Duquette [28]. Ti6Al4V alloy was experimentally investigated by Mall and coworkers [29,30]. These analyses show that fretting fatigue life or strength decreases with increase in contact Hertzian peak pressure. However, among these results data points are too few to reflect the complete picture of contact pressure effect. The investigation of high strength steel by Lee et al. [31] and the investigation of 7075-T6 aluminum alloy by Adibnazari and Hoeppner [32] prove the existence of a normal pressure threshold, increasing the pressure above which does not affect the life, in fretting fatigue when the contact pressure is large enough. Fernando et al. [33] reported the variation of fretting fatigue life with contact stress for BS L65 4% Cu–Al alloy. At low contact pressure, fretting fatigue life decreases with increase in contact pressure whereas at high contact pressure fretting fatigue life increases with increase in contact pressure. Furthermore, the fretting fatigue life of Al–Mg–Si alloy 6061 exhibits a minimum and a maximum with increase in contact pressure. With increase in contact pressure, fretting fatigue life decreases, shows a minimum at 100 MPa contact pressure and

* Corresponding author. Tel.: +86 1082313240.
E-mail address: guoqingwu@buaa.edu.cn (G.Q. Wu).

http://dx.doi.org/10.1016/j.wear.2014.12.033
0043-1648/

then increases, reaches a maximum at an intermediate contact pressure of 150 MPa and thereafter decreases [34].

A variety of testing devices have been developed to study different hardware configurations and service components [34–36]. However, little or no standardization has been made to allow comparison of test results between various existing test systems. Therefore, fretting fatigue testing results might be different (even opposite) to each other. For example, Naidu and Raman [34] reported for one kind of aluminum alloy (AA6061) that the fretting fatigue life exhibited a variable behavior with increase in the contact pressure. With a different kind of testing device, Benhamena et al. [36] reported for another aluminum alloy (5086H24), which is similar to AA6061 in composition and properties, that the fretting fatigue life increased with the increase of contact force. Among different kinds of testing devices, the ring-type is widely used for its simple structure, easy operation, low cost and good generalization. However, there are still some problems which need to be paid enough attention to, such as low accuracy, poor stability and the effect of its self-weight. To this end, a loading device was designed in this study, which solved the problem that part of load was unapplied due to vibration. It also eliminated the impact of the self-weight of the device. Thus, the device has substantially increased the accuracy and reliability for the fretting fatigue test, and has enabled testing condition closer to actual working condition [37].

Suh and coworkers [38,39] advanced the delamination theory which was based on the behavior of dislocations at the surface, subsurface crack and void formation, and subsequent joining of cracks by shear deformation of the surface in the 1970s. It indicates that, under fretting condition, plastic deformation and damage are accumulated below the contact surfaces and then caused strain hardening. Thin flake-shaped debris particles were then generated by a process of subsurface delamination occurring via cracks which originated from hard particles within the deformed zones (but not at the contact surface) and propagated parallel to the surface. Furthermore, some cracks may propagate perpendicularly to the surface and become the fatigue crack. The delamination theory provided the theoretical foundation for fatigue crack nucleation. According to literature, a large fraction of the life, approximately 80–90% of total life, is generally spent in crack nucleation and only a very small fraction of the life is spent in crack propagation to a critical size under high cycle fatigue [40,41]. Thus, we will pay much attention to the fatigue crack initiation area.

Table 1
Composition of Ti-1023 titanium alloy.

Element	V	Fe	Al	O	N	C	H	Ti
wt%	9–11	1.6–2.2	2.6–3.4	< 0.13	< 0.05	< 0.05	< 0.010	Balance

Table 2
Tensile properties of Ti-1023 titanium alloy at room temperature.

Property	Tensile strength σ_b/MPa	Yield strength $\sigma_{p_{0.2}}$/MPa	Elongation δ_5/%	Reduction of area ψ/%
Value	1123	1059	15.3	64.4

Contact pressure and stress evolve during fretting tests in general, and this will obviously affect the evolution of fatigue damage leading to nucleation. In the work of Ding et al. [42], for example, the evolution of contact scars for titanium alloy (Ti6Al4V) is presented for gross slip, partial slip and mixed slip regimes. They have made successful prediction of fatigue crack nucleation in fretting, due to fretting-induced wear.

With a new test facility, we have investigated fretting fatigue properties of Ti-1023 titanium alloy at different contact pressure. Both fatigue fracture and fretting scar were analyzed by scanning electron microscopy (SEM). Moreover, the depth of crack origin zone in fatigue fracture has been analyzed quantitatively, to investigate the relationship between this depth and fretting fatigue strength and to identify the mechanism of the contact pressure effect. The emphasis of the paper is on the fatigue crack initiation area and fracture surface analysis.

2. Materials and experiments

Ti-1023 titanium alloy specimens machined from hot rolled bar were used in fretting fatigue and plain fatigue tests. The heat treatment was 755 °C for 2 h, water cooling, and then 530 °C for 8 h, air cooling. The composition of Ti-1023 titanium alloy is shown in Table 1, and the tensile properties at room temperature are shown in Table 2. Commercial 30CrMnSiA high strength structural steel was used as fretting pad material, which was heated to 880 °C, oil cooled, and then tempered at 540 °C for 1 h, water cooled. The composition of 30CrMnSiA high strength structural steel is shown in Table 3. One aim of the research is to simulate the practical case of helicopter hub sleeves, where the materials involved are the combination of steel and the titanium alloy. The choice of the steel was made to match this real application case. The geometry of the fretting fatigue specimen and the fretting pad with bridge-type were shown in a previous publication [37]. The gage parts of the fretting fatigue specimen and the fretting pad required $R_a \leq 0.8$ μm surface conditions, and both of them were degreased with acetone.

The fretting fatigue tests were performed using PLG-100 computerized high-frequency push–pull fatigue testing machine. They were carried out according to HB 5287-1996 standard, using a sinusoidal wave at frequency of 74–80 Hz, stress ratio of 0.1, in atmospheric condition and room temperature with fretting pad pressed onto specimen to simulate fretting condition. The fretting fatigue strength was defined as the maximum cyclic stress (σ_{max}), throughout this paper. Five levels of contact pressure, namely 3 MPa, 5 MPa, 10 MPa, 20 MPa, and 45 MPa, were considered. The contact pressure was in plane–plane contact state, and applied using the loading device specifically designed by the authors. The fretting fatigue testing system is shown in Fig. 1. The high strength spring was used to load, which solved the problem that part of load was unapplied due to vibration in the case of screw loading. Digital force measurement device was used to monitor contact pressure, which assured the accuracy. The proving ring on the fatigue testing machine with supporting arm eliminated the influence of its self-weight, and made the laboratory condition closer to actual working condition. The observation of fracture surface of fretting fatigue and the fretting area was carried out using a JSM-5800 scanning electron microscope (SEM).

Table 3
Composition of 30CrMnSiA high strength structural steel.

Element	C	Si	Mn	P	S	Cr	Fe
wt%	0.28–0.34	0.90–1.20	0.80–1.10	≤ 0.025	≤ 0.025	0.80–1.10	Balance

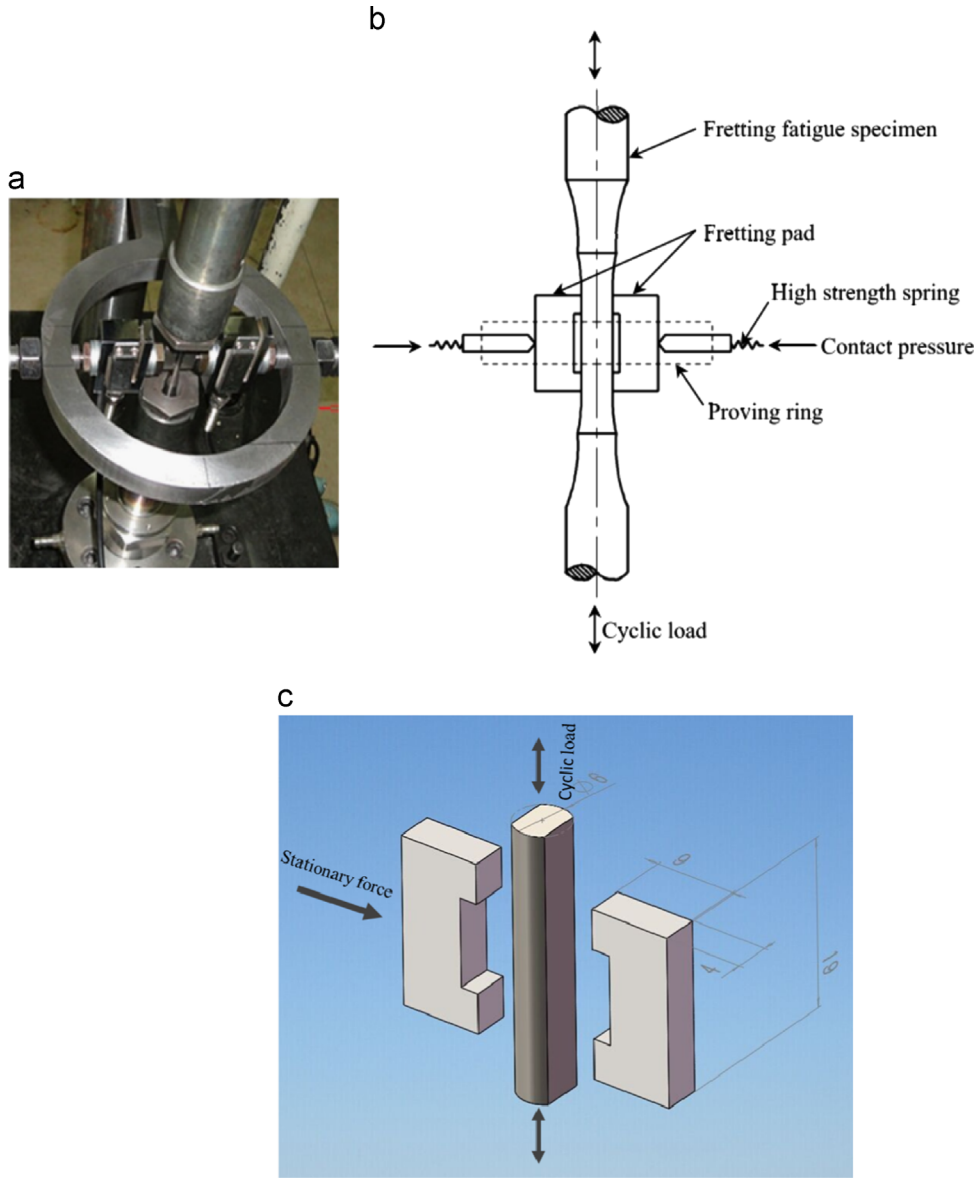

Fig. 1. Fretting fatigue testing system. (a) Photo of loading device; (b) schematic drawing of fretting fatigue test; and (c) schematic of flat-on-flat specimen arrangement.

Fig. 2. Photographs showing the wear damaged areas before fracture, after 10^7 cycles. Contact pressure 3 MPa, 5 MPa, 10 MPa, 20 MPa, and 45 MPa from left to right.

An even distribution of contact pressure was intended in the design. Although the fretting bridge and the fatigue specimen had plane–plane contact mode, during operation there was not complete

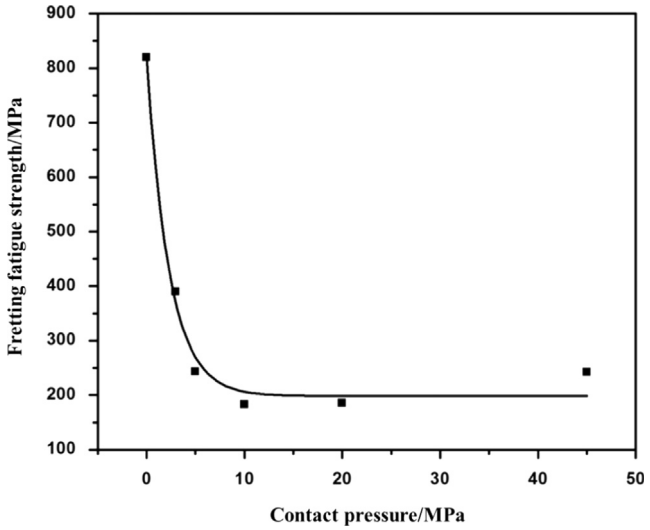

Fig. 3. The effect of contact pressure on fretting fatigue strength of Ti-1023 titanium alloy.

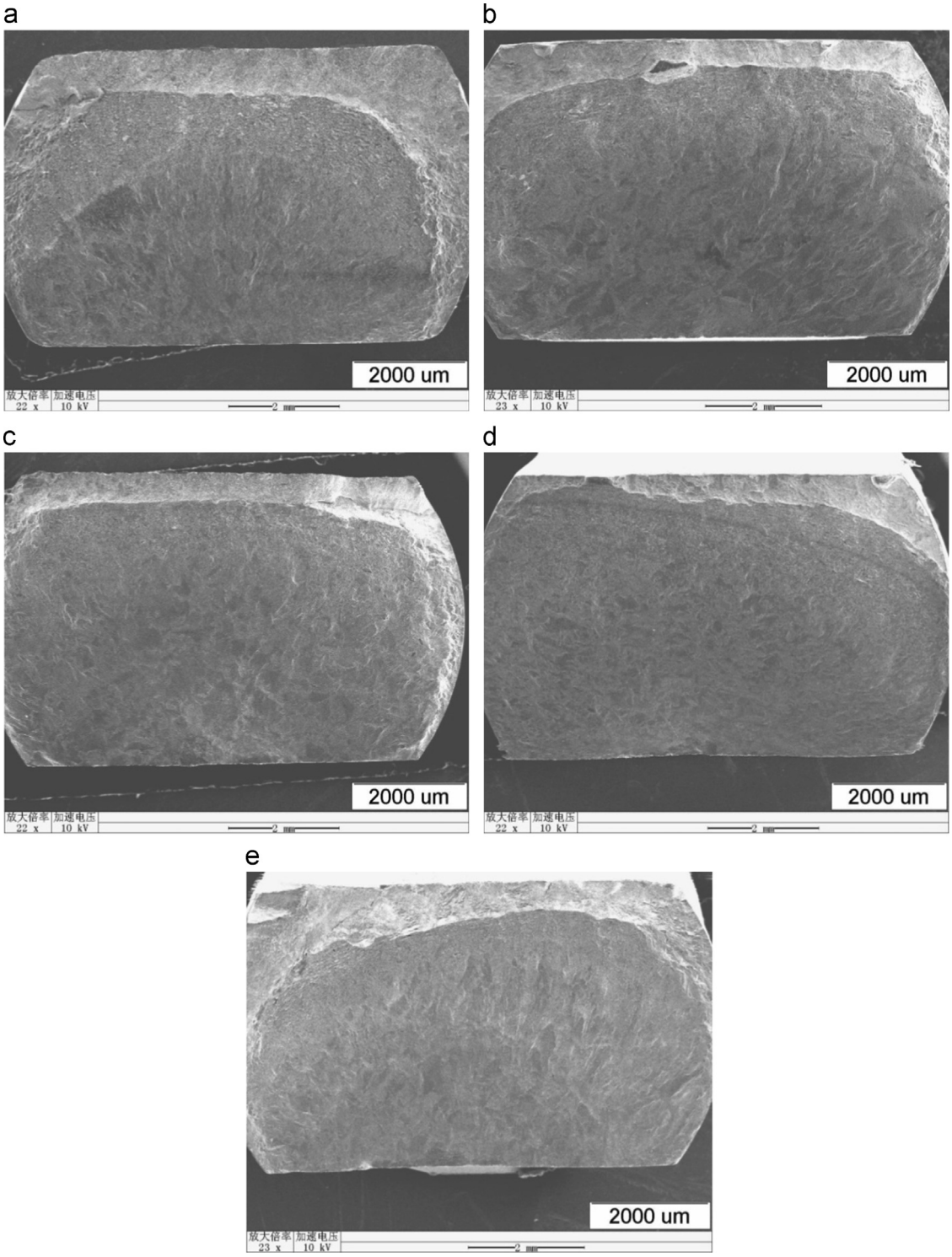

Fig. 4. Fracture morphology of fatigue crack propagation area at different contact pressure. (a) $F=3$ MPa ($N=371{,}208$); (b) $F=5$ MPa ($N=363{,}050$); (c) $F=10$ MPa ($N=471{,}917$); (d) $F=20$ MPa ($N=347{,}432$); and (e) $F=45$ MPa ($N=347{,}673$).

contact between the two, partly due to surface roughness and curvature. Only some areas had contact and thus the fretting wear damage (Fig. 2). This means that the real contact stress is larger than the nominal contact pressure quoted. However, Fig. 2 shows that the size of the wear damaged area does not change significantly with the increase of the contact load. As there is a large range of contact load applied, the changing trend of the actual contact stress is similar to the changing trend of the contact pressure.

3. Results

3.1. Fretting fatigue strength at different contact pressure

Fig. 3 shows the relationship between the fretting fatigue strength of Ti-1023 titanium alloy and contact pressure. It can be seen that the fatigue strength drops rapidly with the effect of fretting, to only 47% of plain fatigue strength when the contact pressure is 3 MPa and 31% of

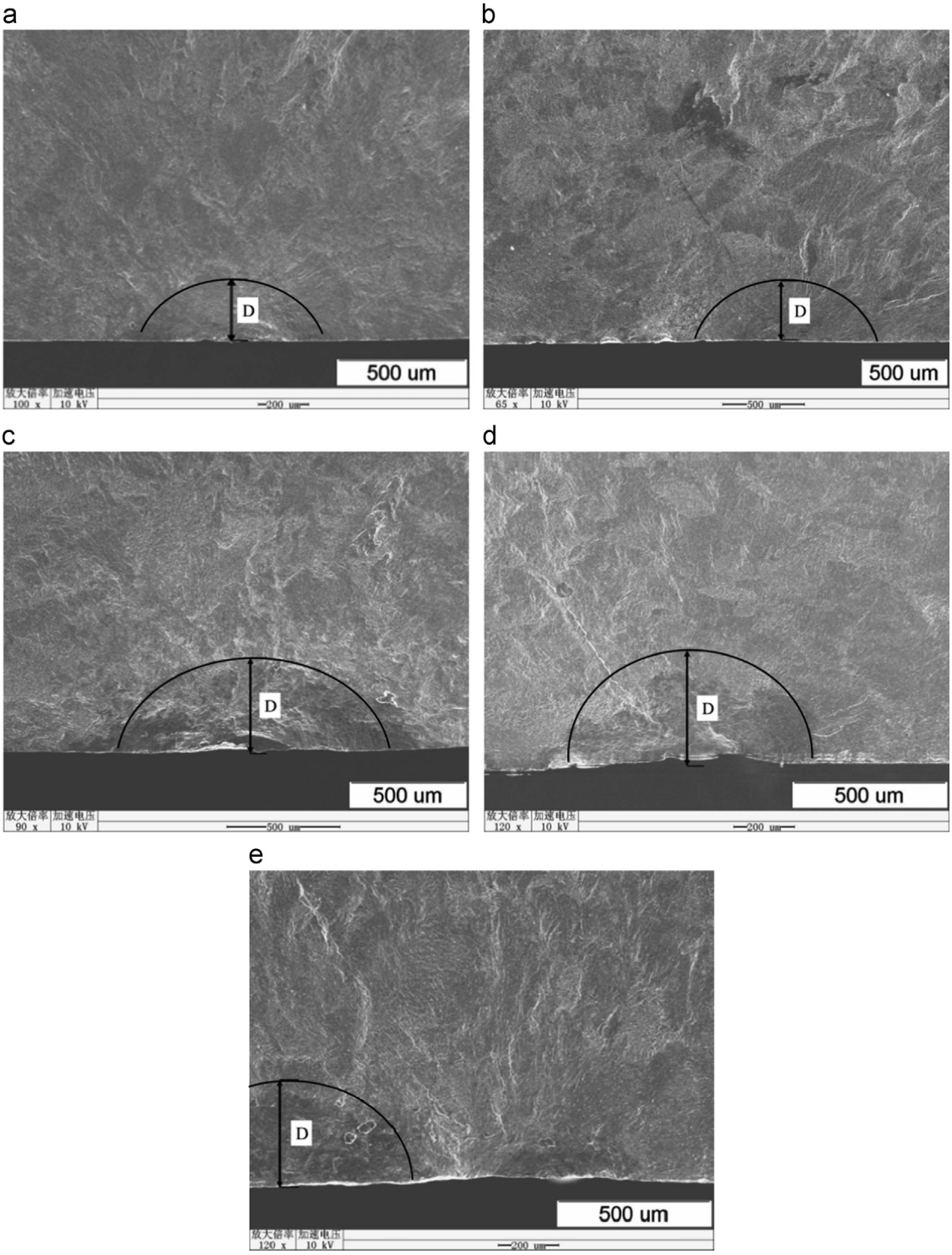

Fig. 5. Fracture morphology of fatigue crack initiation area at different contact pressure. (a) $F=3$ MPa ($N=371{,}208$); (b) $F=5$ MPa ($N=363{,}050$); (c) $F=10$ MPa ($N=471{,}917$); (d) $F=20$ MPa ($N=347{,}432$); and (e) $F=45$ MPa ($N=347{,}673$).

plain fatigue strength when the contact pressure is 5 MPa. The presence of fretting has an enormous impact on the fatigue strength of Ti-1023 titanium alloy. The fretting fatigue strength remains constant (about 200 MPa) after the contact pressure increases to 10 MPa.

3.2. *Fretting fatigue fracture morphology at different contact pressure*

Fig. 4 shows the fretting fatigue fracture morphology of Ti-1023 titanium alloy at different contact pressure, which is composed by three typical areas similar to plain fatigue fracture: (I) the fatigue crack initiation area, (II) the crack propagation area, and (III) the instant rupture area. The cracks all initiate from the fretting area of fatigue specimens, and then expand to the inner material radially. The crack initiation area usually in the shape of a half circle or a half oval is smoother, flatter and darker than the crack propagation area and the instant rupture area. The crack propagation area has the characteristic of fatigue striation and occupies a large proportion of the fatigue fracture surface. The instant rupture area is rough, small and has a shear lip appearance. Moreover, the

Table 4
Depth of crack initiation area at different contact pressure.

Contact pressure (MPa)	Depth of crack initiation area (μm)
3	240
5	360
10	410
20	380
45	360

roughness of the fretting fatigue fracture increases with increasing contact pressure.

After comparing fretting fatigue fracture morphology in five contact pressure levels, we find that there is generally no difference among them in terms of the sizes of crack propagation area and instant rupture area. The main difference is in the crack initiation area. Following the objective to investigate the relationship between the crack initiation area and contact pressure, we define the depth of the fatigue crack initiation area (D), according

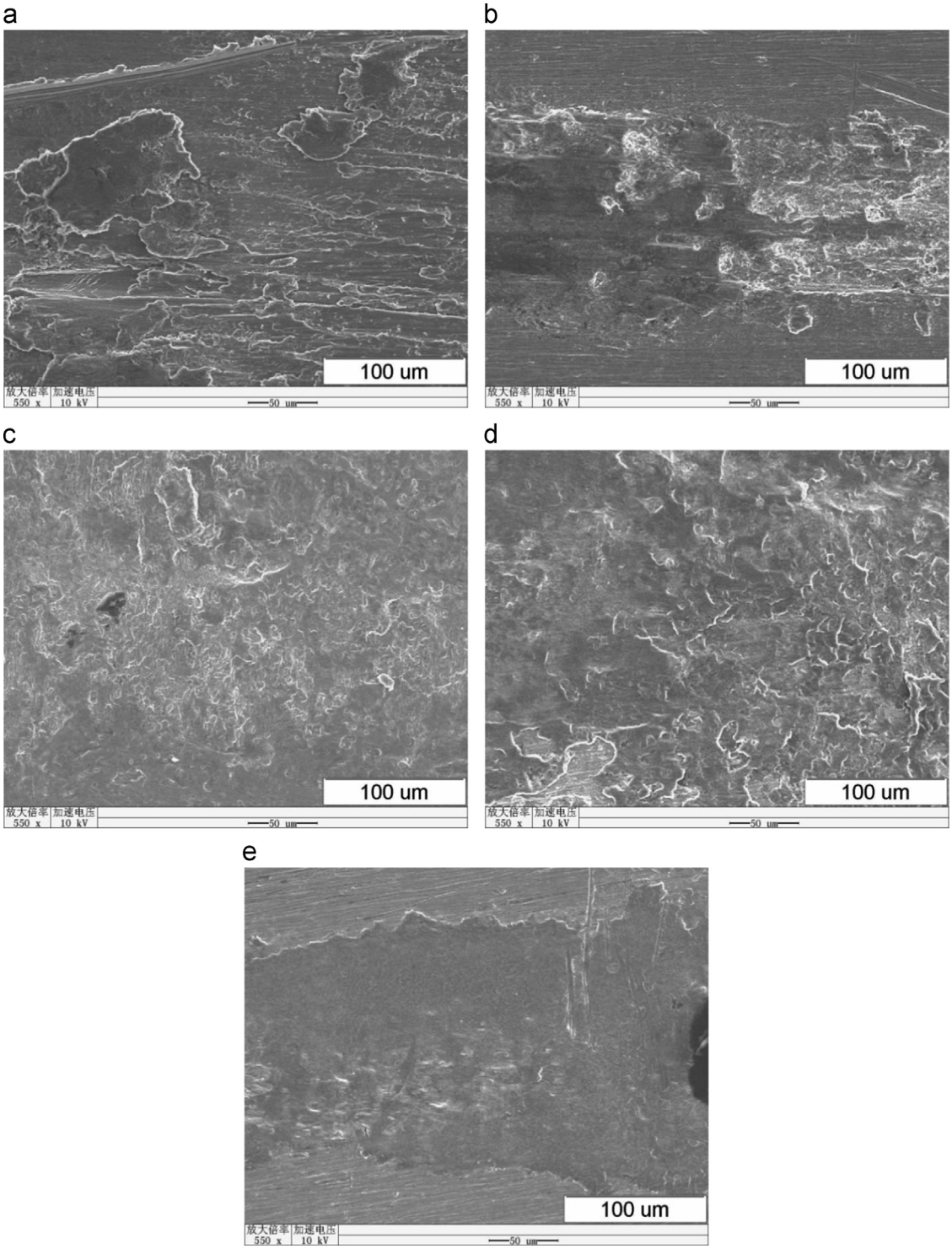

Fig. 6. Fretting area morphology of fretting fatigue specimens at different contact pressure. (a) F=3 MPa; (b) F=5 MPa; (c) F=10 MPa; (d) F=20 MPa; and (e) F=45 MPa.

to the characteristics described here. Fig. 5 shows the measurement of the depth of the fatigue crack initiation area (D) at different contact pressure. Table 4 gives these values. No attempt was made to distinguish it from the zone under high compressive stresses due to the contact stresses, from a microscopical point of view. The microscopical features of the latter are unclear. Ref. [37] shows the microhardness profile beneath the contact zone and the depth of the zone where the profile is different from the rest of the specimen is 0.4 mm, the same range of depth as the initiation depth listed in Table 4.

3.3. Fretting area morphology of fretting fatigue specimen at different contact pressure

Fretting area morphology after cleaning of fretting fatigue specimens in different contact pressure levels is shown in Fig. 6. As we can see, fretting makes serious damages to fatigue test specimens and the main damage patterns are fatigue flake and plow. At contact pressure of 3–5 MPa, the size of fatigue flakes adhering to fretting fatigue specimen is big and the plow is clear. At contact pressure of 10–20 MPa, the size of fatigue flakes diminishes, the number of fatigue flakes drops and the plow becomes indistinct. At contact pressure of 45 MPa, both fatigue flakes and plow disappear.

4. Discussion

4.1. Relationship between the fretting fatigue strength and the depth of crack initiation area

Fig. 7 shows the relationship between the fretting fatigue strength and the depth of crack initiation area of the Ti-1023 titanium alloy. We can see that the depth of crack initiation area increases rapidly with the increase of contact pressure when the contact pressure is smaller than 10 MPa. At the same time, the fatigue strength for fretting fatigue drops rapidly. This means that there is a strong correlation between the depth of crack initiation area and the fretting fatigue strength. Contact pressure influences fatigue strength through influencing the initiation of fatigue crack. Once fatigue crack initiation area is formed, contact pressure plays little part in the development of fretting fatigue.

4.2. Effects of the contact pressure

Delamination wear is a common wearing mechanism in titanium alloy. According to the delamination theory [38,39], cracks originate from hard particles and then propagate parallel to the surface to form flake-shaped debris. Furthermore, some cracks may propagate perpendicularly to the surface and become the fatigue crack. Research by Wu et al. [37] and Everitt et al. [43] has shown that fretting action caused strong surface hardening in the contact area of titanium alloys. In Ti6Al4V titanium alloy, the debris layer is thicker at larger normal load [43]; in Ti-1023 titanium alloy, strain hardening up to 400 μm below the fretting surface is caused by fretting [37]. Everitt et al. presented detailed analysis of fretting wear debris for titanium alloy in the context of understanding fatigue and cyclic damage in titanium alloys [43]. Cracks initiate deeper and propagate faster due to strain hardening with increasing contact pressure when the contact pressure between fretting pad and fatigue specimen is small.

When the contact pressure is relatively large, flake-shaped debris are squashed into small parts which cannot be discharged by vibration and eventually form “third body”. The third body avoids the direct contact between fretting pad and fatigue specimen and prevents larger fretting fatigue damage happening to the surface. So, the fretting area is smoother with less fatigue flakes and plow as shown in Fig. 6(e). This balances the effect of large cracks' initiation depth and propagation rate. It is these combined effects that result in the measured relationship between fretting fatigue strength and contact pressure.

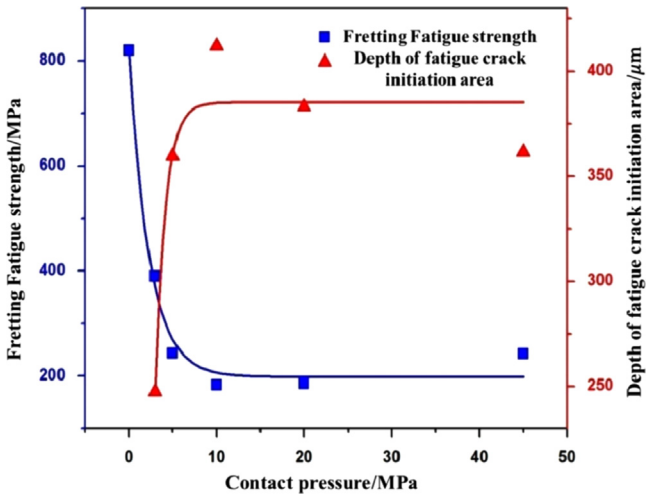

Fig. 7. Fretting fatigue strength and the depth of fatigue crack initiation area of Ti-1023 titanium alloy with increasing contact pressure.

Future work will be carried out to investigate experimentally the depth of strain hardening zone caused by fretting at different contact pressure, to verify our proposed mechanism in this article. The relationship between the depth of strain hardening zone and the depth of fatigue crack initiation area will be investigated, too.

5. Conclusion

The fretting fatigue strength drops rapidly with the increase of contact pressure at low contact pressure levels (smaller than 10 MPa), at only 31% of plain fatigue limit when the contact pressure is 5 MPa. At contact pressure of 10–45 MPa, the fatigue strength has no significant change.

All the cracks initiate from the fretting area of fretting fatigue specimen. The depth of crack initiation area increases rapidly with the increase of contact pressure at low contact pressure levels (smaller than 10 MPa), and then remains stable. The changing trends of the depth of crack initiation area and the fretting fatigue strength are in the opposite directions. This means that there is a strong correlation between the depth of crack initiation area and the fretting fatigue strength. The fatigue strength decreases with the increase of the depth of crack initiation area.

The main damage patterns are fatigue flake and plow. At low contact pressure, the size of fatigue flakes is big and the plow is clear. With the increase of the contact pressure, the size of fatigue flakes diminishes, the number of fatigue flakes reduces, and the plow becomes indistinct.

References

[1] A. Drechsler, T. Dörr, L. Wagner, Mechanical surface treatments on Ti–10V–2Fe–3Al for improved fatigue resistance, Mater. Sci. Eng. A 243 (1998) 217–220.
[2] S.K. Jha, K.S. Ravichandran, Effect of mean stress (stress ratio) and aging on fatigue-crack growth in a metastable beta titanium alloy, Ti–10V–2Fe–3Al, Metall. Mater. Trans. A 31 (2000) 703–714.
[3] R.A. Antoniou, T.C. Radtke, Mechanisms of fretting-fatigue of titanium alloys, Mater. Sci. Eng. A 237 (1997) 229–240.
[4] D.L. Anton, M.J. Lutian, L.H. Favrow, D. Logan, B. Annigeri. Effects of contact stress and slip distance on fretting fatigue damage in Ti–6Al–4V/17-4 PH

contacts, in: Symposium on Fretting Fatigue: Current Technology and Practices, Salt Lake City, 1998: pp. 119–140.
[5] M.M. Hamdy, R.B. Waterhouse, The fretting fatigue behaviour of Ti–6Al–4V at temperatures up to 600 °C, Wear 56 (1979) 1–8.
[6] Olof Vingsbo, Staffan Söderberg, On fretting maps, Wear 126 (1988) 131–147.
[7] S. Fayeulle, P. Blanchard, L. Vincent, Fretting behavior of titanium alloys, Tribol. Trans. 36 (1993) 267–275.
[8] Rebecca Cortez, Shankar Mall, Jeffrey R. Calcaterra, Investigation of variable amplitude loading on fretting fatigue behavior of Ti–6Al–4V, Int. J. Fatigue 21 (1999) 709–717.
[9] T.E. Matikas, E. Shell, P.D. Nicolaou, Characterization of fretting fatigue damage using nondestructive approaches, Proc. SPIE Int. Soc. Opt. Eng. 3585 (1999) 2–10.
[10] K. Iyer, S. Mall, Analyses of contact stress and stress amplitude effects on fretting fatigue life, J. Eng. Mater. Technol. 123 (1) (2001) 85–93.
[11] T.A. Venkatesh, B.P. Conner, S. Suresh, A.E. Giannakopoulos, T.C. Lindley, C.S. Lee, An experimental investigation of fretting fatigue in Ti–6Al–4V: the role of contact conditions and microstructure, Metall. Mater. Trans. A 32 (2001) 1131–1146.
[12] J.M. Wallace, R.W. Neu, Fretting fatigue crack nucleation in Ti–6Al–4V, Fatigue Fract. Eng. Mater. Struct. 26 (2003) 199–214.
[13] J. Takeda, M. Niinomi, T. Akahori, Effect of microstructure on fretting fatigue and sliding wear of highly workable titanium alloy, Ti–4.5Al–3V–2Mo–2Fe, Int. J. Fatigue 26 (2004) 1003–1015.
[14] S. Mall, S.A. Namjoshi, W.J. Porter, Effects of microstructure on fretting fatigue crack initiation behavior of Ti–6Al–4V, Mater. Sci. Eng. A 383 (2004) 334–340.
[15] H. Lee, S. Mall, Fretting fatigue and stress relaxation behaviors of shot-peened Ti–6Al–4V, J. ASTM Int. 2 (2005) JAI12031.
[16] H. Lee, S. Mall, J.H. Sanders, S.K. Sharma, Wear analysis of Cu–Al coating on Ti–6Al–4V substrate under fretting condition, Tribol. Lett. 19 (2005) 239–248.
[17] Hyukjae Lee, Shankar Mall, Jeffrey H. Sanders, Shashi K. Sharma, Russell S. Magaziner, Characterization of fretting wear behavior of Cu–Al coating on Ti–6Al–4V substrate, Tribol. Int. 40 (2007) 1301–1310.
[18] Patrick J. Golden, Michael J. Shepard, Life prediction of fretting fatigue with advanced surface treatments, Mater. Sci. Eng. A 468–470 (2007) 15–22.
[19] J.J. Madge, S.B. Leen, I.R. McColl, P.H. Shipway, Contact-evolution based prediction of fretting fatigue life: effect of slip amplitude, Wear 262 (2007) 1159–1170.
[20] J.J. Madge, S.B. Leen, P.H. Shipway, The critical role of fretting wear in the analysis of fretting fatigue, Wear 263 (2007) 542–551.
[21] J.J. Madge, S.B. Leen, P.H. Shipway, A combined wear and crack nucleation–propagation methodology for fretting fatigue prediction, Int. J. Fatigue 30 (2008) 1509–1528.
[22] G.H. Majzoobi, K. Azadikhah, J. Nemati, The effects of deep rolling and shot peening on fretting fatigue resistance of Aluminum-7075-T6, Mater. Sci. Eng. A 516 (2009) 235–247.
[23] O.J. McCarthy, J.P. McGarry, S.B. Leen, Microstructure-sensitive prediction and experimental validation of fretting fatigue, Wear 305 (2013) 100–114.
[24] Janne Juoksukangas, Arto Lehtovaara, Antti Mäntylä, The effect of contact edge geometry on fretting fatigue behavior in complete contacts, Wear 308 (2013) 206–212.
[25] J. Vázquez, C. Navarro, J. Domínguez, Analysis of the effect of a textured surface on fretting fatigue, Wear 305 (2013) 23–35.
[26] M.J. Dobromirski, Variables of Fretting Process: are there 50 of them, 60, ASTM: Standardization of fretting fatigue test methods and equipment, Philadelphia, 1992.
[27] K. Endo, H. Goto, Initiation and propagation of fretting fatigue cracks, Wear 38 (1976) 311–324.
[28] D.J. Gaul, D.J. Duquette., The effect of fretting and environment on fatigue crack initiation and early propagation in a quenched and tempered 4130 steel, Metall. Trans. A 11 (1980) 1555–1561.
[29] H. Lee, S. Mall, Effect of dissimilar mating materials and contact force on fretting fatigue behavior of Ti–6Al–4V, Tribol. Int. 37 (2004) 35–44.
[30] K. Iyer, S. Mall, Effects of cyclic frequency and contact stress on fretting fatigue under two-level block loading, Fatigue Fract. Eng. Mater. Struct. 23 (2000) 335–346.
[31] Sung-Keun Lee, Kozo Nakazawa, Masae Sumita, Norio Maruyama, Effects of contact load and contact curvature radius of cylinder pad of fretting fatigue in high strength steel, ASTM Spec. Tech. Publ. 1367 (2000) 199–212.
[32] Saeed Adibnazari, David W. Hoeppner, A fretting fatigue normal pressure threshold concept, Wear 160 (1993) 33–35.
[33] U.S. Fernando, G.H. Farrahi, M.W. Brown, Fretting fatigue crack growth behaviour of BS L65 under constant normal load, ESIS 18 (1994) 183–195.
[34] N.K.R. Naidu, S.G.S. Raman, Effect of contact pressure on fretting fatigue behaviour of Al–Mg–Si alloy AA6061, Int. J. Fatigue 27 (2005) 283–291.
[35] A. Hutson, H. Lee, S. Mall, Effect of dissimilar metals on fretting fatigue behavior of Ti–6Al–4V, Tribol. Int. 39 (2006) 1187–1196.
[36] A. Benhamena, A. Amrouche, A. Talha, N. Benseddiq, Effect of contact forces on fretting fatigue behavior of bolted plates: numerical and experimental analysis, Tribol. Int. 48 (2012) 237–245.
[37] G.Q. Wu, Z. Li, W. Sha, H.H. Li, L.J. Huang, Effect of fretting on fatigue performance of Ti-1023 titanium alloy, Wear 309 (2014) 74–81.
[38] S. Jahanmir, N.P. Suh, Mechanics of subsurface void nucleation in delamination wear, Wear 44 (1977) 17–38.
[39] J.R. Fleming, N.P. Suh, The relationship between crack propagation rates and wear rates, Wear 44 (1977) 57–64.
[40] Shantanu A. Namjoshi, S. Mall, V.K. Jain, O. Jin, Fretting fatigue crack initiation mechanism in Ti–6Al–4V, Fatigue Fract. Eng. Mater. Struct. 25 (2002) 955–964.
[41] J. Meriaux, S. Fouvry, K.J. Kubiak, S. Deyber, Characterization of crack nucleation in TA6V under fretting–fatigue loading using the potential drop technique, Int. J. Fatigue 32 (2010) 1658–1668.
[42] J. Ding, G. Bandak, S.B. Leen, E.J. Williams, P.H. Shipway, Experimental characterisation and numerical simulation of contact evolution effect on fretting crack nucleation for Ti–6Al–4V, Tribol. Int. 42 (2009) 1651–1662.
[43] N.M. Everitt, J. Ding, G. Bandak, P.H. Shipway, S.B. Leen, E.J. Williams, Characterisation of fretting-induced wear debris for Ti–6Al–4V, Wear 367 (2009) 283–291.